



The combined nomogram based on the CT features may be used as a complementary method of frozen sections to predict invasive lung adenocarcinoma manifesting as ground-glass nodules

Yangyang Sun^{1#}, Bin Wang^{2#}, Ke Bi^{3#}, Xue Meng¹, Lei Zhang⁴, Xiwen Sun²

¹Department of Radiology, Shanghai East Hospital, Tongji University School of Medicine, Shanghai 200120, China; ²Department of Radiology, Shanghai Pulmonary Hospital, Tongji University School of Medicine, Shanghai 200433, China; ³Department of Pathology, Tongji Hospital, Tongji University School of Medicine, Shanghai 200065, China; ⁴Department of Radiology, Shanghai General Hospital, Shanghai Jiao Tong University School of Medicine, Shanghai 200080, China

Contributions: (I) Conception and design: X Sun, Y Sun, L Zhang; (II) Administrative support: X Sun, L Zhang; (III) Provision of study materials or patients: B Wang, K Bi; (IV) Collection and assembly of data: X Meng, Y Sun; (V) Data analysis and interpretation: Y Sun, B Wang, K Bi; (VI) Manuscript writing: All authors; (VII) Final approval of manuscript: All authors.

[#]These authors contributed equally to this work.

Correspondence to: Xiwen Sun, PhD. Department of Radiology, Shanghai Pulmonary Hospital, Tongji University School of Medicine, 507 Zhengmin Road, Shanghai 200433, China. Email: sunxiwen5256@163.com; Lei Zhang, PhD. Department of Radiology, Shanghai General Hospital, Shanghai Jiao Tong University School of Medicine, 85 Wujin Road, Shanghai 200080, China. Email: zhanglei4302@vip.sina.com.

Background: Frozen sections (FS) deferral sometimes occurs in the intraoperative pathological classification of early lung adenocarcinoma, which is not conducive to the decision-making of surgical treatment. Here, we compared the predictive performance of the combined nomogram based on the computer tomography (CT) features with FS to investigate whether the nomogram could be used as a complementary method for FS when FS deferral occurs to predict invasive adenocarcinoma (IAC) manifesting as ground-glass nodules (GGNs) during surgery.

Methods: In this study, 205 early lung adenocarcinomas manifesting as GGNs from 178 patients who had undergone surgical treatment were included and divided into a training set (n=123) and a validation set (n=82). The training set defined a hybrid nomogram incorporating CT features and intraoperative measured tumor size based on multivariate logistic regression to predict IAC, and the validation set was used to verify the predictive performance. We also collected the diagnostic results of FS and compared the predictive performance of the established nomogram with FS.

Results: The accuracy of combined nomogram in predicting IAC in the training and validation sets was 91.1% and 89.0%, respectively, and the predictive accuracy of FS in the training set and validation set was 87.0% and 86.6%, respectively. The predictive accuracy between the combined nomogram and FS have no significant difference.

Conclusions: Compared with FS, the performance of the combined nomogram in predicting the lung IAC manifesting as GGNs is satisfactory, which has the potential to be used as a complementary method for FS when FS deferrals during surgery.

Keywords: Nomogram; frozen section (FS); spiral computed tomography; lung neoplasms; forecasting

Submitted Jan 08, 2020. Accepted for publication Mar 06, 2020.

doi: 10.21037/jtd.2020.03.75

View this article at: <http://dx.doi.org/10.21037/jtd.2020.03.75>

Introduction

Lung cancer remains the leading cause of cancer incidence and mortality worldwide (1), and adenocarcinoma is the dominant histological type of lung cancer (2,3). According to the new classification, lung adenocarcinoma was classified as atypical adenomatous hyperplasia (AAH), adenocarcinoma in situ (AIS), minimally invasive adenocarcinoma (MIA) and IAC (4). With the popularization of high resolution CT, the detection rate of pulmonary nodules is rapidly increasing. The GGNs were one of the types of the pulmonary nodules, and a large part of them were identified as early lung adenocarcinoma (5-7). The diagnosis of IAC is of great significance to the surgical treatment, which can determine whether a patient is suitable for limited resection or lobe resection (8). Currently, the FS is the key guide for the intraoperative pathological classification of early lung adenocarcinoma. However, FS deferrals (i.e., FS can't give clear and timely diagnosis but wait for the result of postoperative paraffin sections) often occurs in the clinical work due to the sampling problems, poor FS quality or whatever other reasons, which may lead to the inappropriate surgery strategy for patients (9,10). It is necessary to find another method that can serve as a complementary intraoperative classification approach for FS.

The CT features, such as the solid part diameter, nodules diameter and CT value, play the important role in the prediction of the pathological classification of early lung adenocarcinoma manifesting as GGNs (11-16). Besides, intraoperative measured tumor size is also an important reference for the pathological staging of lung adenocarcinoma, a study demonstrated that the intraoperatively measured tumor size and FS results should be considered jointly to predict the final pathological classification for early lung adenocarcinoma (17). As an effective method of risk prediction, a nomogram can integrate different predictive factors and display the predictive results clearly and intuitively, so doctors can easily use it and explain the predictive results to patients. Therefore, nomogram is widely researched and used as an aid to decision-making in clinical practice (18-21).

In this study, we established a combined nomogram based on CT features to predict IAC during surgery, which may work as a complementary intraoperative pathological classification method when FS deferrals. To our knowledge, no relevant studies have explored a new approach that

serves as a complementary diagnostic method for FS.

Methods

Patients

The institutional review board of The Shanghai Pulmonary Hospital approved this retrospective study and the Medical Ethics Committee waived the requirements for patients' informed consent. One hundred seventy eight patients with 205 early lung adenocarcinoma who underwent surgery from January 2018 to August 2018 were enrolled in this study.

The inclusion criteria were as follows: (I) CT examination performed within one month before surgery; (II) the maximum diameter of tumor were ≤ 2 cm; (III) the preoperative CT layer thickness was less than 2 mm; (IV) the peripheral lung adenocarcinoma. The exclusion criteria were: (I) the CT image had obvious artifacts around the tumor; (II) use of the contrast medium (at present, most of the patients with GGNs are checked with the chest CT without contrast medium, so the CT images used the contrast medium of a small number of patients were excluded to reduce the confounding factors). All the patient's clinical information (e.g., gender, age) was also collected. The flowchart of this study is shown in *Figure 1*.

CT image acquisition

The preoperative chest CT examination of all patients performed in full inspiration to eliminate artifacts of respiratory movement. The scanner Somatom Definition AS (Siemens Medical Systems, Germany) used at an efficient dose of 120 kV tube energy and 200 mAs to scan CT images. The parameters the scanner used were as follows: the detector width of 64 mm \times 0.625 mm, pitch of 1.0, and a matrix of 512 \times 512. CT images were reconstructed with a layer thickness of 1.0 or 2.0 mm, an increment of 0.7 mm and a standard soft kernel (Siemens B31 filter, Siemens Medical Solutions, Forchheim, Germany).

Measurement of conventional CT features

The measurement of the CT features of all cases was firstly measured by the radiologist (Y Yang, with 5 years of experience in chest imaging) and reviewed by another radiologist (XW Sun, with 20 years of experience in chest imaging). Both the radiologists were aware of

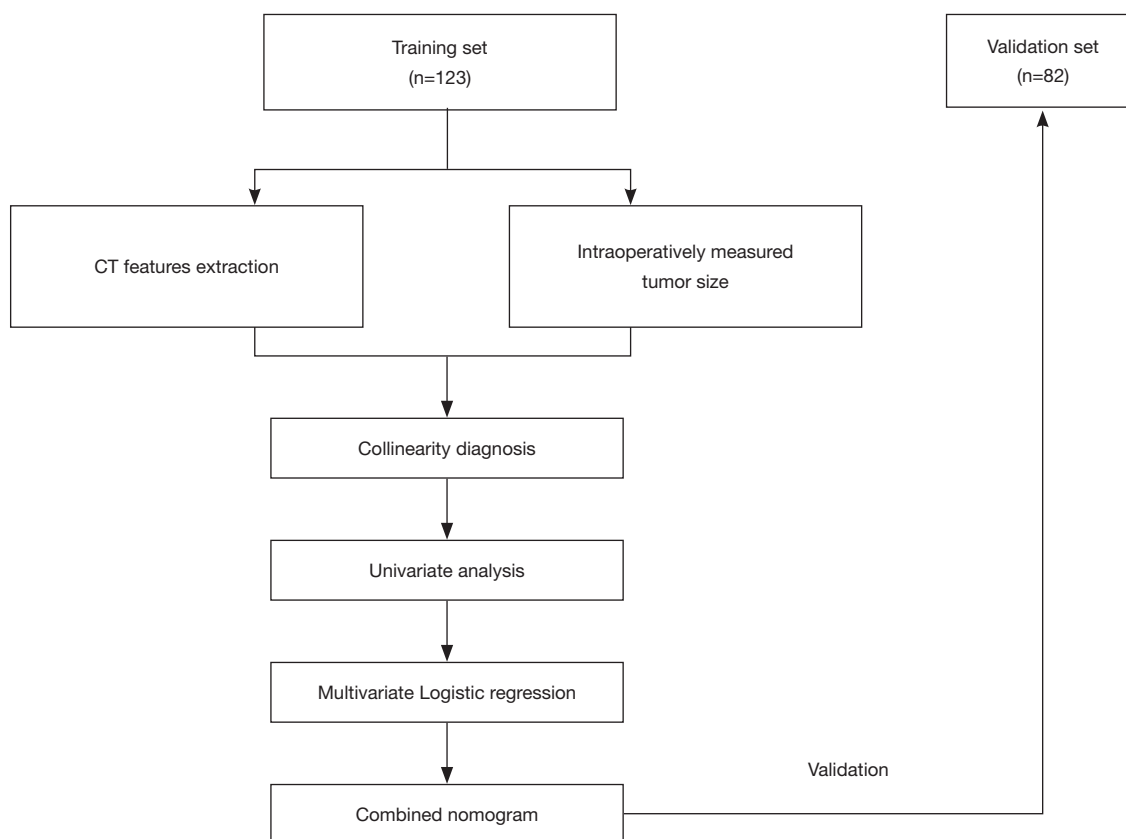


Figure 1 Study flowchart.

that which nodules in CT image were identified as lung adenocarcinoma, but were unknown of pathological classification of the nodules. The measurement of CT features of the GGNs was based on the recommendations for measuring pulmonary nodules at CT from the Fleischner Society (22). Solid part diameter, solid part proportion, CT long diameter, CT short diameter, mean CT value, maximum CT value and variance of CT value were measured at the maximum cross-section of the tumors on a lung window (window level, -450; window width, 1,500) by the radiologists in the medical imaging workstation. The measurement of volume was conducted using 3D slicer software (version 4.8.1), the border of the nodules was manually performed by a radiologist (Y Yang) and reviewed by another radiologist (XW Sun). Intraoperatively tumor size was immediately measured at the largest diameter of the specimen by pathologists after the tumor tissue was resected by a thoracic surgeon.

In addition, some important radiological signs (including vacuole sign, spiculation, lobulation, pleural retraction) were also collected by a radiologist (Y Yang) and reviewed by another radiologist (XW Sun).

The estimation of the reproducibility of CT features measurement

The estimation of the intra-observer and inter-observer reproducibility of CT features extraction was done by the ICC (intra-class and inter-class correlation coefficients). We randomly selected 30 cases from all the nodules to assess the reproducibility of CT features measurement. The CT features reproducibility was also performed by two radiologists (Radiologist 1: Y Yang, Radiologist 2: XW Sun). Radiologist 1 measured the CT features of those selected 30 cases again after one week. If the ICC is greater than 0.75, we think the consistency of CT features measurement is

well-achieved (23).

FS and paraffin sections diagnoses

Results of intraoperative FS diagnosis and postoperative paraffin sections diagnosis were collected. In the majority of the cases, two pathologists (Y Huang, LP Zhang, thoracic pathologists with the work experience of more than 10 years) could reach an agreement about the diagnosis, and the third senior pathologist (CY Wu, thoracic pathologist with work experience of more than 20 years) was invited to obtain a negotiated diagnosis for the remaining debatable cases. For each case, the specimen was diagnosed according to the classification the International Association for the Study of Lung Cancer/American Thoracic Society/European Respiratory Society of lung adenocarcinoma. The paraffin section diagnosis was considered as the final diagnosis in this study.

Construction and validation of the prediction nomogram

The collinearity diagnosis of all the features was conducted using the variance inflation factor (VIF) and Tolerance value if the VIF >10 or the Tolerance value <0.05, we thought that the collinearity existed. We selected the predictive factors to forecast IAC through the univariate and multivariate logistic regression analysis in the training set, and then a combined nomogram was constructed based on multivariate logistic regression analysis. Confirmation of the diagnostic performance of the established predictive nomogram was finally carried out in the validation set. The calibration curve and relative operating characteristic (ROC) curve were plotted and the areas under the ROC curve (AUC) value of the predictive nomogram in training and validation sets was calculated. To further test the diagnostic performance and clinical usefulness of the combined nomogram, we compared the diagnostic accuracy of the nomogram and FS.

Statistical analysis

Quantitative data was described as mean \pm SD or median (25th–75th); qualitative data was described as n (%). The comparisons between groups for qualitative variables were performed by Chi-square test or Fisher exact test and comparisons between groups for quantitative variables was performed using a *t*-test or Wilcoxon test. The likelihood ratio test with backward step-down selection was used for

the multivariate logistic analysis. The VIFs and Tolerance value were calculated using the “car” package. The ROC curves were plotted using the “pROC” package. Nomogram construction and calibration plots were performed using the “rms” package. A two-sided P value <0.05 was considered statistically significant. The cut-off probability threshold of the nomogram for the prediction of IAC was determined by maximizing the Youden index. The statistical analysis was conducted using R statistical software (version 3.3.1) and SPSS software for Windows, version 20.0 (IBM, Armonk, NY, USA).

Results

Clinical characteristics

According to the inclusion and exclusion criteria, from January 2018 to August 2018, 205 early lung adenocarcinomas of 178 patients were included in this study, including 17 cases of AAH, 67 cases of AIS, 70 cases of MIA and 51 cases of IAC (see some examples in *Figure 2*). By random sampling method with a ratio of 3:2, 123 cases (10 AAH, 40 AIS, 42 MIA, and 31 IAC) were divided into training set and 82 cases (7 AAH, 27 AIS, 28 MIA and 20 IAC) into validation set. All the cases were split into a non-IAC and IAC groups in the training and validation sets. Finally, the training set consisting of 92 non-IAC cases and 31 IAC cases (total: 123 cases), the validation set consisting of 62 non-IAC cases and 20 IAC cases (total: 82 cases). The basic information of all nodules is shown in *Table 1*.

The estimation of the reproducibility of CT features measurement

The intra-observer ICCs and inter-observer ICCs of the CT features measurement of the randomly selected 30 cases were all greater than 0.75, indicating that the CT feature measurements had good reproducibility so that all the selected CT features were included in the following analysis.

Construction and validation of the combined nomogram

First, in the collinearity diagnosis (*Table S1*), the three features were excluded (including solid part proportion, Maximum CT value, and short diameter) in this analysis process. The remaining features were included into the univariate logistic regression analysis, and five features

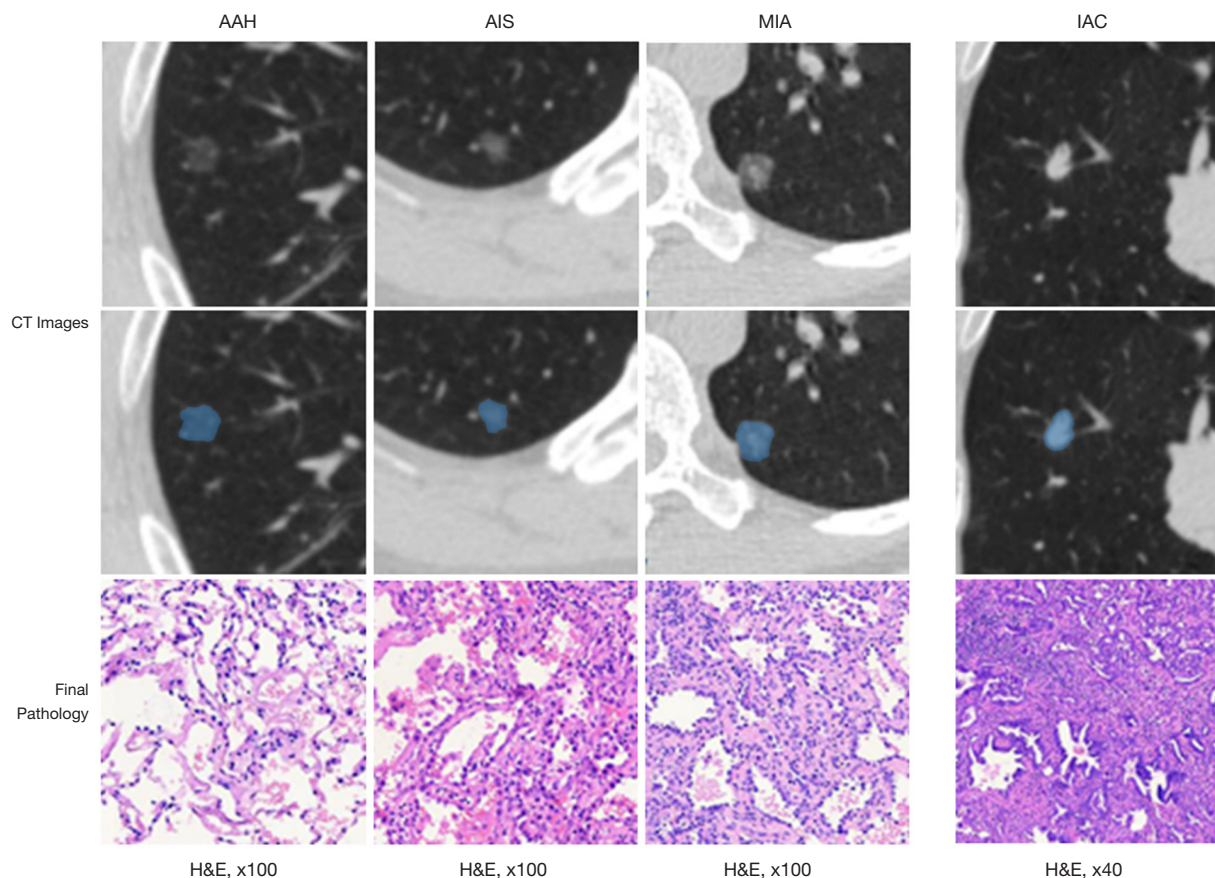


Figure 2 Examples in the data set of nodules. The blue shadow represent the shape of the lesions. The final pathology is the diagnosis of postoperative paraffin sections. The CT images and paraffin sections [hematoxylin and eosin (H&E), $\times 100$ for AAH, AIS and MIA, hematoxylin and eosin (H&E), $\times 40$ for IAC] are AAH, AIS, MIA and IAC respectively. AAH, atypical adenomatous hyperplasia; AIS, adenocarcinoma in situ; MIA, minimally invasive adenocarcinoma; IAC, invasive adenocarcinoma.

were excluded, including gender, vacuole sign, speculation, lobulation, pleural retraction. Finally, age, intraoperatively measured size, solid part diameter and mean CT value were identified as the independent predictors of IAC by multivariate logistic regression analysis (Table 2). The predictive multivariate logistic regression equation is blow:

$$\ln\left(\frac{P}{1-P}\right) = -5.700 + 0.106 * \text{Age}$$

+0.390 * Solid part diameter

+0.011 * Mean CT value

+0.269 * Intraoperatively measured tumor size

In the equation, P is the predictive odds of IAC. The established combined nomogram incorporating selected features based on multivariate logistic regression analysis in

training set and confirmed in the validation set (Figure 3).

The performance of the predictive nomogram

The calibration curve of the nomogram is shown in Figure 3, showing that the combined nomogram has good calibration capability for the training set, and the calibration curve in the validation set was similar to that of the training set. The AUC value of the established nomogram is shown in Figure 4. The AUC of the nomogram in training set and the validation set was 0.942 (95% CI, 0.898–0.987) and 0.954 (95% CI, 0.912–0.996), respectively. Compared with training set, the predictive performance of the nomogram in the validation set had no significantly reduce. Both calibration curves and ROC curves showed that our combined nomogram performed well in both the training

Table 1 Clinical characteristics of patients in training set and validation set

Variables	Training set			Validation set		
	Non-IAC (n=92)	IAC (n=31)	P	Non-IAC (n=62)	IAC (n=20)	P
Age (years)	51.5±11.3	60.0±10.1	<0.001	48.7±11.7	60.7±9.9	<0.001
Gender, n (%)			0.097			0.629
Male	29 (31.5)	5 (16.1)		19 (30.6)	5 (25.0)	
Female	63 (68.5)	26 (83.9)		43 (69.4)	15 (75.0)	
Nodule type, n (%)			<0.001			<0.001
PGGNs	48 (52.2)	2 (6.5)		36 (58.1)	2 (10.0)	
MGGNs	44 (47.8)	29 (93.5)		26 (41.9)	18 (90.0)	
Vacuole sign	6 (6.5)	5 (16.1)	0.263	6 (9.7)	1 (5.0)	1
Spiculation	2 (2.2)	3 (9.7)	<0.05	3 (4.8)	4 (20.0)	<0.05
Lobulation	14 (15.2)	9 (29.0)	0.161	8 (12.9)	5 (25.0)	0.288
Pleural retraction	8 (8.7)	6 (19.4)	0.432	7 (11.3)	2 (10.0)	1
Solid part diameter	0 (0, 4.2)	6.9 (5.2,8.5)	<0.001	0 (0, 4.1)	6.2 (5.4, 7.9)	<0.001
Solid part proportion	0 (0, 4.6)	0.45 (0.36, 0.61)	<0.001	0 (0, 0.50)	0.45 (0.39, 0.56)	<0.01
Intraoperatively tumor size	7.0 (6.0, 10.0)	13.0 (10.0, 15.0)	<0.001	7.0 (5.0, 8.0)	15.0 (10.0, 16.0)	<0.001
CT long diameter	11.5 (9.4, 14.0)	16.0 (13.3, 18.6)	<0.001	10.5 (9.1, 12.3)	16.3 (13.3, 18.4)	<0.001
CT short diameter	8.0 (6.6, 9.3)	11.4 (9.5, 14.2)	<0.001	7.1 (5.8, 8.8)	10.6 (8.8, 11.7)	<0.001
Mean CT value	-593.4 (-641.3, -561.4)	-464.7 (-550.6, -400.8)	<0.001	-604.2 (-652.5, -541.6)	-483.4 (-553.0, -382.4)	<0.001
Maximum CT value	-418.6 (-513.0, -343.0)	-163.7 (-264.0, -59.0)	<0.001	-455.5 (-545.0, -302.8)	-181.5 (-294.8, -52.8)	<0.001
Variance of CT value	107.1 (-83.7, 126.6)	171.7 (147.6, 197.8)	<0.001	101.3 (74.7, 130.8)	162.3 (138.3, 189.5)	<0.001
Volume	451.0 (271.3, 670.4)	1,795.3 (736.8, 2,304.7)	<0.001	296.4 (209.3, 573.7)	1,544.9 (9,35.3, 1,960.6)	<0.001

Qualitative variables are described as n (%), quantitative variables are described as mean ± SD or median (25th–75th). P<0.05 was considered statistically significant. Mean CT value, maximum CT value and variance of CT value were measured in the largest circle within the lesion at the maximum cross-section by the radiologists. Intraoperatively tumor size was immediately measured by pathologists after the tumor tissue was resected by a thoracic surgeon. IAC, invasive lung adenocarcinoma; Non-IAC indicates atypical adenomatous hyperplasia, adenocarcinoma *in situ* and minimally invasive adenocarcinoma; PGGNs, pure ground-glass nodules; MGGNs, mixed ground-glass nodules.

and validation sets, indicated that the combined nomogram had a good and stable application value for IAC prediction during surgery.

The comparison between the nomogram and FS

The Confusion Matrix of the FS and nomogram prediction results is shown in *Table 3*. In the training set, 10 non-IACs were overestimated and 6 IACs underestimated by FS, 6

non-IACs were overestimated and 5 IACs underestimated by the combined nomogram. The situation is similar in the validation set, 5 non-IACs were overestimated and 6 IACs underestimated by FS, and 7 non-IACs were overestimated and 2 IACs underestimated by combined nomogram. The results of the comparison between the nomogram and FS are shown in *Table 4*. The accuracy, sensitivity, specificity, positive predictive value (PPV) and negative predictive value (NPV) of the nomogram and FS for the prediction

Table 2 Independent predictors of the IAC diagnoses

Predictors	Univariate analysis			Multivariate analysis		
	OR	95 % CI	P	OR	95 % CI	P
Age	1.081	1.033–1.131	<0.05	1.112	1.027–1.204	<0.01
Solid part diameter	1.865	1.471–2.364	<0.001	1.478	1.118–1.953	<0.01
Intraoperatively tumor size	1.522	1.298–1.784	<0.001	1.309	1.067–1.606	<0.05
Mean CT value	1.016	1.010–1.022	<0.001	1.011	1.003–1.019	<0.01
Nodule type	15.818	3.564–70.197	<0.001	0.952	0.022–41.764	0.980
Long diameter	1.376	1.207–1.569	<0.001	0.966	0.636–1.467	0.872
Variance of CT value	1.046	1.029–1.064	<0.001	1.024	0.984–1.065	0.240
Volume	1.001	1.001–1.002	<0.001	1.001	0.999–1.003	0.538
Gender	2.394	0.835–6.863	0.104	–	–	–
Vacuole sign	2.123	0.558–8.085	0.270	–	–	–
Spiculation	4.395	0.926–20.866	0.062	–	–	–
Lobulation	2.213	0.718–6.822	0.167	–	–	–
Pleural retraction	1.497	0.547–4.100	0.432	–	–	–

Intraoperatively tumor size was measured by pathologists immediately after the tumor tissue was resected by a thoracic surgeon. Solid part diameter, Long diameter, and Volume were measured by the radiologists in the preoperative CT images. The features which $P < 0.05$ in the univariate analysis were included into the multivariate analysis. IAC, invasive adenocarcinoma; Non-IAC indicates atypical adenomatous hyperplasia, adenocarcinoma *in situ* and minimally invasive adenocarcinoma.

of IAC all surpassed 70%. The predictive accuracy of the nomogram was 91.1% and 89.0% for training and validation sets, respectively, and FS was 87.0% and 86.6% in training and validation sets, respectively. These results showed that the nomogram and the FS had almost the same predictive performance in both the training and validation sets for predicting IAC, indicating that the established nomogram is a reliable approach that can work as a complementary method for FS predicting IAC during surgery.

Discussion

The determination of the optimal surgical resection range for patients with peripheral lung adenocarcinoma requires accurate intraoperative pathological classification, and the discrimination of non-IAC and IAC is especially important. Usually, lobectomy is the choice for IAC, whereas limited resection conducted for non-IAC (8). Although FS can provide timely and accurate classification of early adenocarcinoma in most cases (8,17), how to obtain satisfactory intraoperative pathological classification still face some challenges. There may be errors and deferrals of

FS due to inflammation with reactive atypia, fibrosis/scar, sampling problems, and suboptimal quality of FS sections. One study showed that the FS errors and deferrals were identified in 12.1% and 6.3% of all the cases (9). Another study (10) also found that there were FS deferrals in 32.35% of all the cases with early lung adenocarcinoma, which could lead to inappropriate surgical treatment for patients. It is, therefore, necessary to find another intraoperative method used as a complementary approach to predicting IAC when FS deferral occurs.

The CT measurements including diameter, CT value, and volume, are important and reliable reference for predicting the pathological classification of early lung adenocarcinoma. Many studies have shown that the CT density of high-stage lung adenocarcinoma differs significantly from that of low-stage adenocarcinoma (11-13). The CT diameter is also an important predictive factor for the pathological classification of early lung adenocarcinoma (14-16). The intraoperative measured tumor size reflects the histological size of the tumor, which may be also related to the pathological staging, which has been incorporated into our combined nomogram in the hope of improved

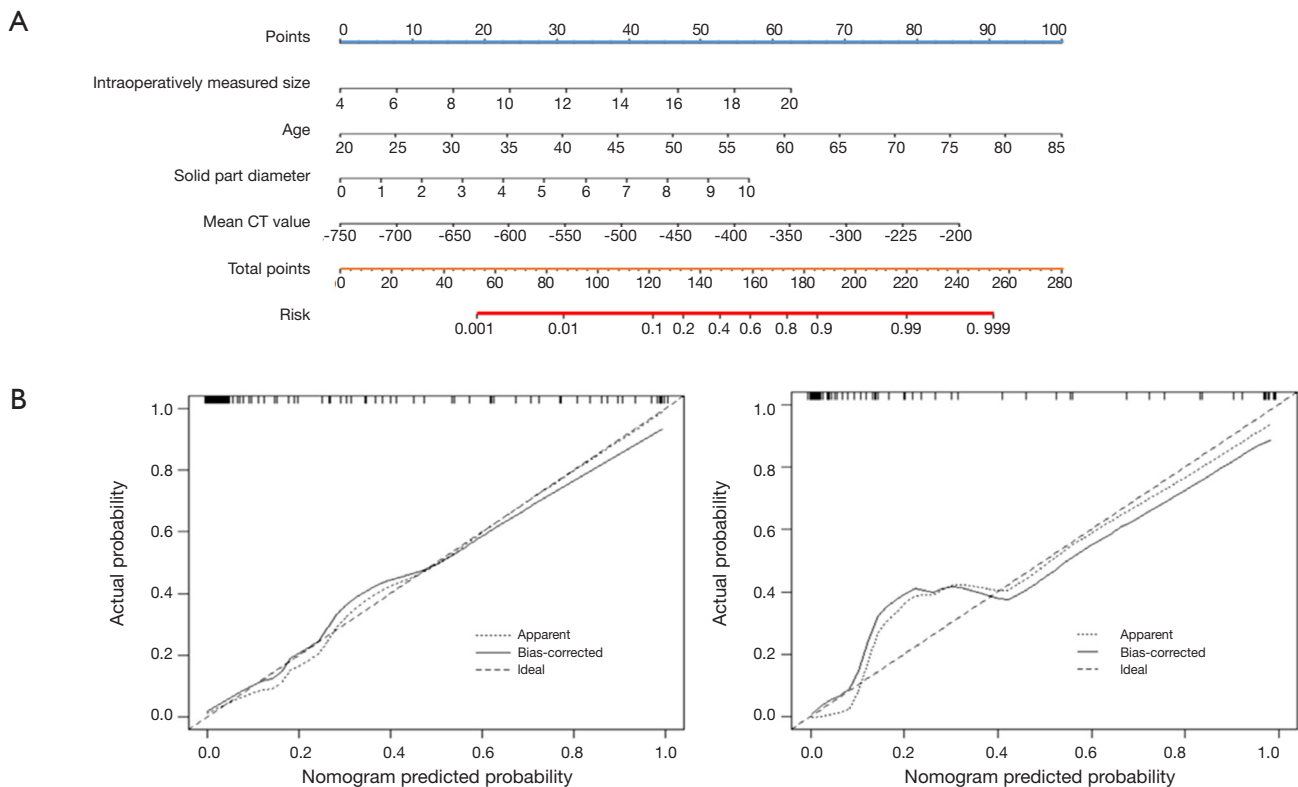


Figure 3 Combined nomogram for the prediction of invasive lung adenocarcinoma (A). Calibration curves of the combined nomogram in the training and validation sets (B). Calibration curve describes the calibration of the nomogram in the consistency between the predicted IAC risks and actual results. The 45° line represents the ideal prediction results, the dotted line represents the actual prediction results of the nomogram, and the solid line represents the bias-corrected prediction results of the nomogram. The closer these two lines are to the ideal line, the better the prediction accuracy of the nomogram will be. IAC, invasive adenocarcinoma.

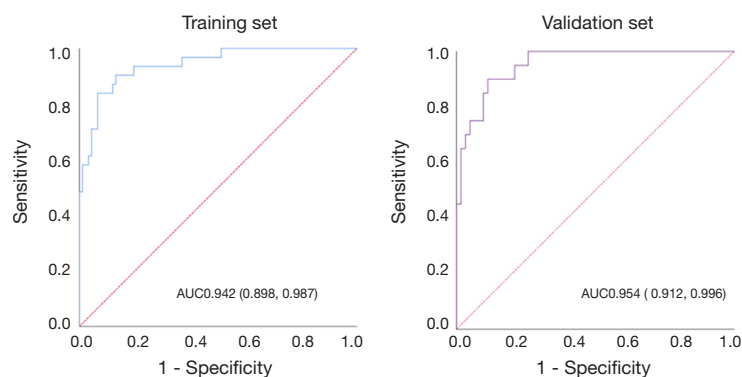


Figure 4 The ROC curves for the diagnosis of the nomogram in training set and validation set. ROC, relative operating characteristic.

intraoperative predictive efficacy. Using a variety of predictors, the nomogram may have ability to quantify the risk of IAC, and its application is simple, intuitive, which has potential to support intraoperative decision-making.

In the training set, the predictive accuracy, sensitivity, specificity, PPV, NPV of our nomogram were 91.1%, 83.9%, 93.5%, 81.3% and 94.5% respectively. In the validation cohort, the accuracy, sensitivity, specificity, PPV,

Table 3 Confusion matrix of the diagnoses of frozen sections and the nomogram

Prediction	Final pathological classification					
	Training cohort			Validation cohort		
	Non-IAC (n=92)	IAC (n=31)	Total (n=123)	Non-IAC (n=62)	IAC (n=20)	Total (n=82)
Frozen sections						
Non-IAC	89.1% [82]	19.4% [6]	88	91.9% [57]	30.0% [6]	63
IAC	10.9% [10]	80.6% [25]	35	8.1% [5]	70.0% [14]	19
Combined nomogram						
Non-IAC	93.5% [86]	16.1% [5]	91	88.7% [55]	10.0% [2]	57
IAC	6.5% [6]	83.9% [26]	32	11.3% [7]	90.0% [18]	25

All values shown as % [n]. IAC, invasive adenocarcinoma; Non-IAC indicates atypical adenomatous hyperplasia, adenocarcinoma *in situ* and minimally invasive adenocarcinoma.

Table 4 Comparison of the diagnostic accuracy of the nomogram and frozen sections

Method	Accuracy (%)	Sensitivity (%)	Specificity (%)	PPV (%)	NPV (%)
Training cohort					
Nomogram	91.1	83.9	93.5	81.3	94.5
Frozen sections	87.0	80.6	89.1	71.4	93.2
Validation cohort					
Nomogram	89.0	90.0	88.7	72.0	96.5
Frozen sections	86.6	70.0	91.9	73.7	90.5

The comparisons were performed in the training and validation sets. IAC, invasive adenocarcinoma; Non-IAC indicates atypical adenomatous hyperplasia; adenocarcinoma *in situ* and minimally invasive adenocarcinoma; PPV, positive predictive value; NPV, negative predictive value.

NPV of the nomogram were 89.0%, 90.0%, 88.7%, 72.0% and 96.5%, respectively. The AUC of the nomogram in training and validation sets were 0.942 (95% CI, 0.898–0.987) and 0.954 (95% CI, 0.912–0.996), respectively. Besides, the calibration curve showed that the combined nomogram had a good calibration ability in both the training and validation sets. These results showed that the combined nomogram not only can accurately predict IAC but also has stable predictive performance.

FS can usually provide an accurate pathological classification for early lung adenocarcinoma, but in some cases, pathologists may give the delayed FS diagnoses due to the poor FS quality, sampling problems or other problems that need to wait for the postoperative paraffin section to provide accurate pathological classification. This, of course, cannot satisfy the time limitation of intraoperative

diagnosis. In this situation, additional tools are required to provide a relatively accurate pathological classification, particularly for the diagnosis of IAC. Encouragingly, the established combination nomogram and FS had almost the same performance for the IAC prediction in the training set and validation set. The predictive accuracy of nomogram and FS in both training and validation sets has surpassed 85%. This has shown that both the nomogram and the FS have good discrimination efficacy of non-IAC and IAC, our nomogram has the potential to give an accurate diagnosis of IAC during surgery when FS deferrals, which may help to make the optimum surgical treatment strategy for patients.

There are some limitations in this study. First, this is a single centered retrospective study that requires external validation data sets to further assess the robustness and practical usefulness of the predictive nomogram.

Secondly, to validate the feasibility of our nomogram as a complementary tool for FS, a data set of the cases with FS deferrals is required. Our future studies will try to overcome these shortfalls in hopes of improving the intraoperative diagnostic accuracy of the pathological classification of early lung adenocarcinoma by jointly using the predictive nomogram and FS, which can help to develop an optimum surgical treatment plan for patients.

In conclusion, the performance of the combined nomogram based on CT features was not inferior to FS in the prediction of IAC, the nomogram has the potential to be used as a complementary method for FS when FS deferrals during surgery. The external validation and the dataset of the cases with FS deferrals are required to confirm the actual application value of the established combined nomogram.

Acknowledgments

Funding: This work was supported by the National Natural Science Foundation of China (Grant number 81872718), Natural Science Foundation of Shanghai (Grant number 19ZR1443100) and Clinical Research Project of Shanghai Pulmonary Hospital (Grant number fk18007).

Footnote

Conflicts of Interest: All authors have completed the ICMJE uniform disclosure form (available at <http://dx.doi.org/10.21037/jtd.2020.03.75>). The authors have no conflicts of interest to declare.

Ethical Statement: The authors are accountable for all aspects of the work in ensuring that questions related to the accuracy or integrity of any part of the work are appropriately investigated and resolved. The study was approved by the institutional review board of The Shanghai Pulmonary Hospital (K18-204Y) and the Medical Ethics Committee waived the requirements for patients' informed consent.

Open Access Statement: This is an Open Access article distributed in accordance with the Creative Commons Attribution-NonCommercial-NoDerivs 4.0 International License (CC BY-NC-ND 4.0), which permits the non-commercial replication and distribution of the article with the strict proviso that no changes or edits are made and the original work is properly cited (including links to both the

formal publication through the relevant DOI and the license). See: <https://creativecommons.org/licenses/by-nc-nd/4.0/>.

References

1. Bray F, Ferlay J, Soerjomataram I, et al. Global cancer statistics 2018: GLOBOCAN estimates of incidence and mortality worldwide for 36 cancers in 185 countries. *CA Cancer J Clin* 2018;68:394-424.
2. Ito H, Matsuo K, Tanaka H, et al. Nonfilter and filter cigarette consumption and the incidence of lung cancer by histological type in Japan and the United States: analysis of 30-year data from population-based cancer registries. *Int J Cancer* 2011;128:1918-28.
3. Casal-Mouriño A, Valdés L, Barros-Dios JM, et al. Lung cancer survival among never smokers. *Cancer Lett* 2019;451:142-9.
4. Travis WD, Brambilla E, Noguchi M, et al. International Association for the Study of Lung Cancer/American Thoracic Society/European Respiratory Society: international multidisciplinary classification of lung adenocarcinoma: executive summary. *Proc Am Thorac Soc* 2011;8:381-5.
5. Sawada S, Komori E, Nogami N, et al. Evaluation of lesions corresponding to ground-glass opacities that were resected after computed tomography follow-up examination. *Lung Cancer* 2009;65:176-9.
6. Kim HJ, Cho JY, Lee YJ, et al. Clinical Significance of Pleural Attachment and Indentation of Subsolid Nodule Lung Cancer. *Cancer Res Treat* 2019;51:1540-8.
7. Wu C, Zhao C, Yang Y, et al. High discrepancy of driver mutations in patients with NSCLC and synchronous multiple lung ground-glass nodules. *J Thorac Oncol* 2015;10:778-83.
8. Liu S, Wang R, Zhang Y, et al. Precise Diagnosis of Intraoperative Frozen Section Is an Effective Method to Guide Resection Strategy for Peripheral Small-Sized Lung Adenocarcinoma. *J Clin Oncol* 2016;34:307-13.
9. Walts AE, Marchevsky AM. Root cause analysis of problems in the frozen section diagnosis of in situ, minimally invasive, and invasive adenocarcinoma of the lung. *Arch Pathol Lab Med* 2012;136:1515-21.
10. He P, Yao G, Guan Y, et al. Diagnosis of lung adenocarcinoma in situ and minimally invasive adenocarcinoma from intraoperative frozen sections: an analysis of 136 cases. *J Clin Pathol* 2016;69:1076-80.
11. Ikeda K, Awai K, Mori T, et al. Differential diagnosis of ground-glass opacity nodules: CT number analysis by

- three-dimensional computerized quantification. *Chest* 2007;132:984-90.
12. Sone S, Hanaoka T, Ogata H, et al. Small peripheral lung carcinomas with five-year post-surgical follow-up: assessment by semiautomatic volumetric measurement of tumor size, CT value and growth rate on TSCT. *Eur Radiol*, 2012;22:104-19.
 13. Zhang YP, Heuvelmans MA, Zhang H, et al. Changes in quantitative CT image features of ground-glass nodules in differentiating invasive pulmonary adenocarcinoma from benign and in situ lesions: histopathological comparisons. *Clin Radiol* 2018;73:504.e9-504.e16.
 14. Cho J, Ko SJ, Kim SJ, et al. Surgical resection of nodular ground-glass opacities without percutaneous needle aspiration or biopsy. *BMC Cancer* 2014;14:838.
 15. Heo EY, Lee KW, Jheon S, et al. Surgical resection of highly suspicious pulmonary nodules without a tissue diagnosis. *Jpn J Clin Oncol* 2011;41:1017-22.
 16. Lim HJ, Ahn S, Lee KS, et al. Persistent pure ground-glass opacity lung nodules ≥ 10 mm in diameter at CT scan: histopathologic comparisons and prognostic implications. *Chest* 2013;144:1291-9.
 17. Zhu E, Xie H, Dai C, et al. Intraoperatively measured tumor size and frozen section results should be considered jointly to predict the final pathology for lung adenocarcinoma. *Mod Pathol* 2018;31:1391-9.
 18. Gittleman H, Sloan AE, Barnholtz-Sloan JS. An independently validated survival nomogram for lower grade glioma. *Neuro Oncol* 2020;22:665-74.
 19. Martini A, Kumarasamy S, Beksac AT, et al. A nomogram to predict significant estimated glomerular filtration rate reduction after robotic partial nephrectomy. *Eur Urol* 2018;74: 833-9.
 20. Oh JR, Park B, Lee S, et al. Nomogram Development and External Validation for Predicting the Risk of Lymph Node Metastasis in T1 Colorectal Cancer. *Cancer Res Treat* 2019;51:1275-84.
 21. Berardi G, Morise Z, Sposito C, et al. Development of a nomogram to predict outcome after liver resection for hepatocellular carcinoma in child-pugh b cirrhosis. *J Hepatol* 2020;72:75-84.
 22. Bankier AA, Macmahon NH, Goo JM, et al. Recommendations for measuring pulmonary nodules at CT: A statement from the Fleischner Society. *Radiology* 2017;285:584-600.
 23. Wu S, Zheng J, Li Y, et al. A radiomics nomogram for the preoperative prediction of lymph node metastasis in bladder cancer. *Clin Cancer Res* 2017;23:6904-11.

Cite this article as: Sun Y, Wang B, Bi K, Meng X, Zhang L, Sun X. The combined nomogram based on the CT features may be used as a complementary method of frozen sections to predict invasive lung adenocarcinoma manifesting as ground-glass nodules. *J Thorac Dis* 2020;12(5):2361-2371. doi: 10.21037/jtd.2020.03.75

Supplementary

Table S1 Collinearity statistics results

Features	Tolerance	VIF
Age	0.736	1.359
Gender	0.902	1.109
Solid part diameter	0.037	27.338
Solid partial proportion	0.038	26.330
Nodule type	0.126	7.908
Vacuole sign	0.828	1.208
Spiculation	0.904	1.106
Lobulation	0.849	1.177
Pleural retraction	0.783	1.276
Intraoperatively tumor size	0.369	2.707
CT long diameter	0.045	22.274
CT short diameter	0.048	20.738
Mean CT value	0.069	14.491
Maximum CT value	0.032	31.090
Variance of CT value	0.045	22.083
Volume	0.110	9.058

Tolerance <0.05 or VIF >10 indicate the existence of the collinearity. VIF, variance inflation factor; CT, computed tomography.